https://doi.org/10.5194/egusphere-2023-1399
Preprint. Discussion started: 12 September 2023

Arctic shoreline displacement with open satellite imagery and data fusion: A pilot study 1984–2022

Tua Nylén[1,2], Mikel Calle[1,3], Carlos Gonzales-Inca[1]

[1]Department of Geography and Geology, University of Turku, Turku, FI-20014, Finland
[2]Department of Geosciences and Geography, University of Helsinki, Helsinki, FI-00014, Finland
[3]Turku Collegium for Sciences, Medicine and Technology (TCSMT), University of Turku, Turku, FI-20014, Finland

Correspondence to: Tua Nylén (tua.nylen@utu.fi)

Abstract. The Arctic coast is facing rapid changes due to thawing permafrost and melting glaciers and sea ice. Communities all around the Arctic urgently need local-scale information on coastal change. This study aimed at developing a scalable and transferable procedure for mapping shoreline displacement in Arctic conditions by using an archive of satellite images. Our approach utilizes cloud computing in Google Earth Engine to process a large number of open satellite images for large areas and a long period of time (here 39 years). The procedure was iteratively developed in two contrasting study areas in Arctic Norway. It applies data fusion (including sensor fusion, algorithm fusion, and decision fusion) to improve classification accuracy and processing efficiency. For one 2 500 km² area of interest, the procedure utilizes c. 600 satellite images to create coastal land cover and shoreline time series in less than one hour. Data fusion reduces problems related to the low availability and quality of satellite data in the Arctic before 2013 and reduces the impacts of noise and short-term changes. However, low data availability tends to create local gaps in the time series. Validation in the Tanafjorden and north-western Svalbard coasts indicates an overall classification accuracy of more than 99 % (against an independent sample of 2000 coastal points) and a median shoreline error distance of less than 15 m (against manually digitized shoreline) in 2019–2022. We exemplify how the method produces new information for identifying coastal change hotspots and examining long-term trends and local scale processes. We give examples of glacier retreat, spit migration, and delta development. This procedure is scalable and transferable to any coastal area demonstrating potential for producing the first circumpolar dataset of shoreline displacement.

1 Introduction

The largest rises in surface temperatures since the beginning of the 20th century have been observed in the Arctic (Serreze & Barry, 2011), making the coast particularly prone to shoreline displacement. Thawing of the permafrost-rich riverbanks decreases their stability, and increased meltwater runoff from glacial watersheds brings more sediments into the coastal system, increasing seaward displacement of the shoreline around those estuaries (Bourriquen et al., 2016). Decreased sea ice and fast ice cover, and a shortening ice period increase wave action and the length of the open water period, leading to accelerated erosion of the coast (Overeem et al., 2011; Barnhart et al., 2014). Thawing of the permafrost-rich coasts

https://doi.org/10.5194/egusphere-2023-1399
Preprint. Discussion started: 12 September 2023

decreases their stability and makes the shoreline more prone to erosion (Lantuit & Pollard, 2008). These processes operate at different spatial and temporal scales and are further impacted by local environmental conditions (Bendixen & Kroon, 2017; Farquharson et al., 2018). Thus, shoreline displacement is associated with large local variation (Are et al., 2008; Bendixen & Kroon, 2017). This kind of spatially varying change is usually impossible to measure with point observations and requires continuous spatial data.

Increased coastal instability is one of the most significant impacts of climate change on the local communities of the Arctic (Barnhart et al., 2014; Radosavljevic et al., 2016; Irrgang et al., 2019). Shoreline displacement has severe consequences for land use, i.e., human settlement, traditional exploitation of raw materials, transport, and cultural heritage (AMAP, 2019; Irrgang et al., 2019). Indigenous peoples of the Arctic are at risk of losing their entire livelihood as, e.g., transport routes and access to fish stocks change dramatically (Larsen & Fondahl, 2014). Settlements as well as sites of cultural and archaeological significance are threatened (Hollesen et al., 2018; Irrgang et al., 2019). In addition, coastal instability may hamper plans for increased economic exploitation of transport routes and mineral resources in the Arctic (Larsen & Fondahl, 2014). Since the intensity of coastal changes will vary locally, the impacts on local communities and the local economy will also be highly variable.

Previous studies have quantified local and regional-scale shoreline displacement rates using remote sensing, which compensates for the lack of direct measurements of shoreline positions (Lantuit et al., 2010, Vos et al., 2019). There are good examples from north-western Canada (e.g., Radosavljevic et al., 2016), north-western Alaska (e.g., Farquharson et al., 2018), western Greenland (Bendixen & Kroon, 2017), Svalbard (e.g., Zagórski et al., 2015), and Laptev Sea (e.g., Günther et al., 2013). However, these studies are often characterized by either a low temporal and spatial resolution (few repeated records and few sites), a short timespan or a small spatial extent. Only a few regional studies of local-scale variability exist (see however, e.g., Farquharson et al., 2018). In addition, the Arctic Coastal Dynamics network (ACD) has made significant efforts to gather pan-Arctic erosion rates by reviewing previous regional studies (Lantuit et al., 2012). Lately, the use of Google Earth Engine for upscaling remote sensing analyses has increased rapidly and made global-scale land cover and coastal analyses feasible (Bishop-Taylor et al., 2021; Li et al., 2021, Pérez-Cutillas et al., 2023).

In optimal conditions, detecting water from multispectral satellite images is a straightforward task since the reflectance of pure, evenly illuminated sea water is very different from the reflectance of land or ice. For example, Ismail and others (2022) and Li and others (2022) reviewed the development and suitability of water extraction methods from satellite remote sensing data. They divided existing methods into threshold segmentation (single-band or multi-band threshold methods) and image classification methods (Li et al., 2022). Threshold segmentation is solely based on the spectral characteristics of water, while image classification can also account for the texture and spatial characteristics (Li et al., 2022). Images can be classified using machine learning methods like support vector machines, decision tree methods, object-based methods, and deep learning (Li et al., 2022). Each of these methods has certain advantages, challenges, and limitations related to, e.g., image noise, water quality, illumination, and opportunities for being automized. A full list of those references on remote sensing of coastal land cover that were used in this study is included in the Supplement.

https://doi.org/10.5194/egusphere-2023-1399
Preprint. Discussion started: 12 September 2023

Supervised classification may help overcome local classification challenges related to water quality or illumination. However, the production of the training data creates an obstacle for automized analyses of large volumes of satellite data over large areas. Data fusion, i.e., utilizing complementary spatial data for creating the training data, might remove this obstacle.

Short-term water level fluctuations have an impact on the location of the instantaneous shoreline at the acquisition time of single images. This greatly influences landcover data extracted from single images, particularly along meso- and macro-tidal coasts (Ding et al., 2021). This phenomenon can be accounted for using tidal corrections, but utilizing dense time series might be even more effective (Laengner et al., 2019; Ding et al., 2021). Time-step decision fusion is a method to summarize time series and extract more robust and accurate information than from individual observations. In our context, it is based on the idea that if the number of observations on each pixel is high enough, we can assume that most water level, weather, and illumination conditions have been observed (c.f. Laengner et al., 2019). Accordingly, we can assume that if we summarize a large number of individual images by, e.g., calculating the median land cover class for each pixel, we will likely get a reliable estimate of the average land cover distribution. Decision fusion also effectively removes noise caused by, e.g., clouds or cloud shadows. Therefore, results from decision fusion are more accurate than those from single images (Laengner et al., 2019).

The aim of this paper was to develop and validate a scalable and transferable procedure for creating long-term time series of Arctic shoreline displacement using open multispectral satellite data. We aimed at describing the final procedure, remaining challenges and limitations, and application examples for coastal geomorphological studies. This is the first and largest step towards producing the first circumpolar map of shoreline displacement.

We iteratively developed a procedure for extracting shoreline displacement data in Google Earth Engine and validated the results using two contrasting study areas in the Norwegian Arctic. During the development process, we examined, e.g., the suitability and availability of satellite image collections, the applicability of different algorithms, the potential of using data fusion, algorithm fusion, and decision fusion, and their impact on the accuracy of the outputs and computing performance.

2 Methods

We developed the procedure for automated extraction of Arctic shoreline displacement time series for 1984–2022 from open-access satellite images, utilizing data fusion and state-of-the-art computing methods. This was an iterative process where the performance was examined, and the outputs were validated against independent data after each iteration. Two types of outputs were created in the process: a time series dataset of coastal land cover (land and sea; raster data) and a time series of shorelines (vector data).

The main components of the procedure were calibrated in one study area, while the final iterations were validated in two study areas. The iterations aimed at answering these questions: Which open multispectral satellite image collections are suitable for extracting useful shoreline information? Does data fusion using complementary open spatial data improve the

https://doi.org/10.5194/egusphere-2023-1399
Preprint. Discussion started: 12 September 2023

efficiency and accuracy of shoreline detection? Which bands and multispectral indices provide useful information for shoreline detection? Do multispectral indices or supervised classification perform better in detecting the shoreline, and does this depend on local environmental conditions? Does algorithm fusion improve the accuracy of shoreline detection? Can decision fusion across several images be used to reduce noise and the impact of short-term sea level fluctuations? What is the overall accuracy of the land cover classification (land and sea) and shoreline extraction, and how do they depend on local environmental conditions? Which processing, performance, or classification challenges remain? How can the time series be summarized to provide meaningful information about the hotspots of shoreline displacement and local geomorphological processes? Considering the remaining errors and output resolution, do the results provide new, meaningful information for examining local geomorphological processes?

The final, proposed procedure for creating time series of coastal landcover and shorelines without user input can be divided into nine steps (Figure 1) that are described in detail in the Supplement.

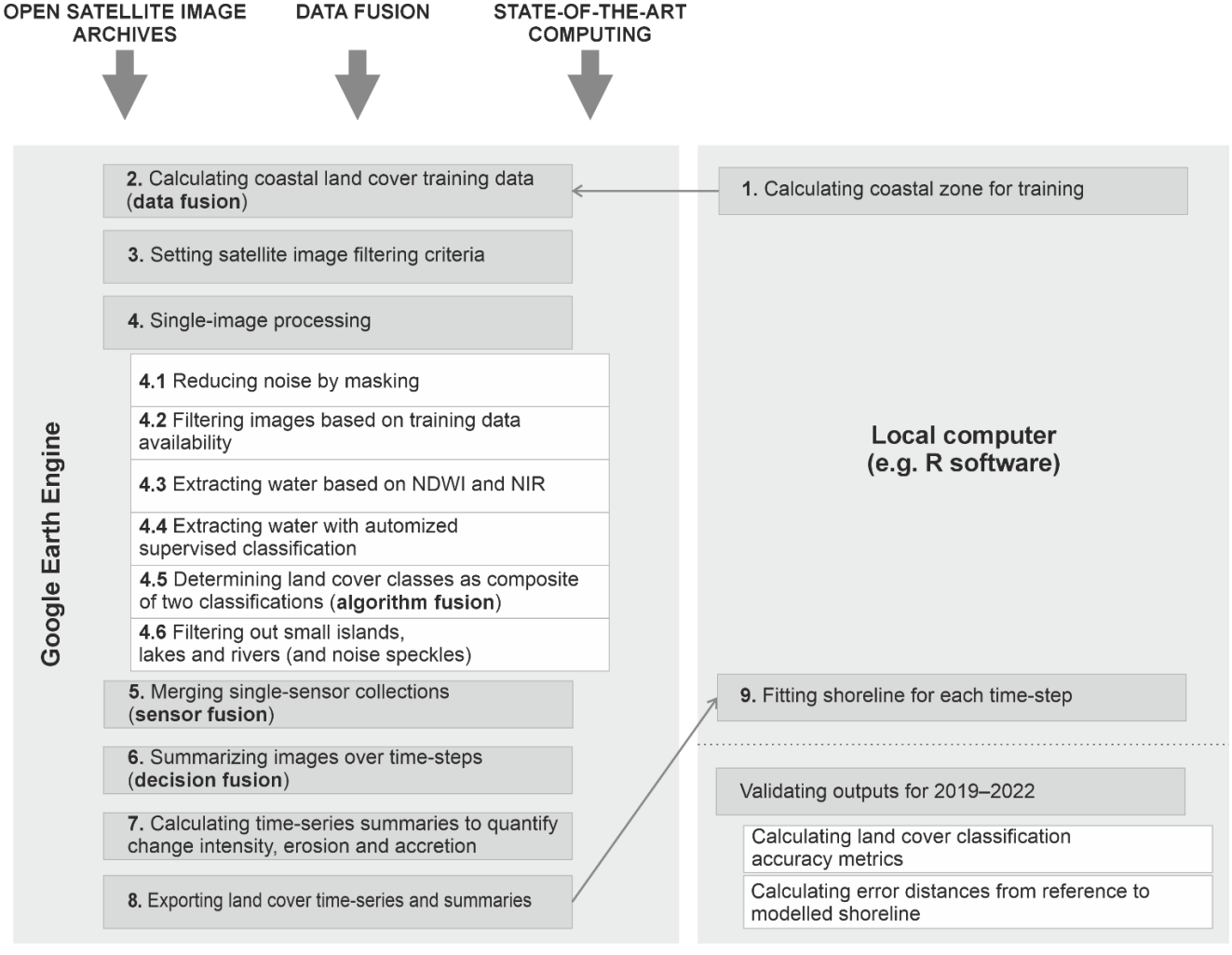

Figure 1. Overview of the proposed procedure, divided into nine steps and followed by validation of the results.

https://doi.org/10.5194/egusphere-2023-1399
Preprint. Discussion started: 12 September 2023

2.1 Study areas

We used two contrasting coastal environments in the European Arctic to calibrate and validate the procedure for extracting shoreline displacement time series. First, the procedure was iteratively calibrated, tested, and validated in the Tanafjorden area, on the Barents Sea coast of Norway (Figure 2). Second, the final procedure was validated in the Ny-Ålesund area at the Greenland Sea coast of the Svalbard archipelago (Figure 2). The two study areas are described in detail in the Supplement.

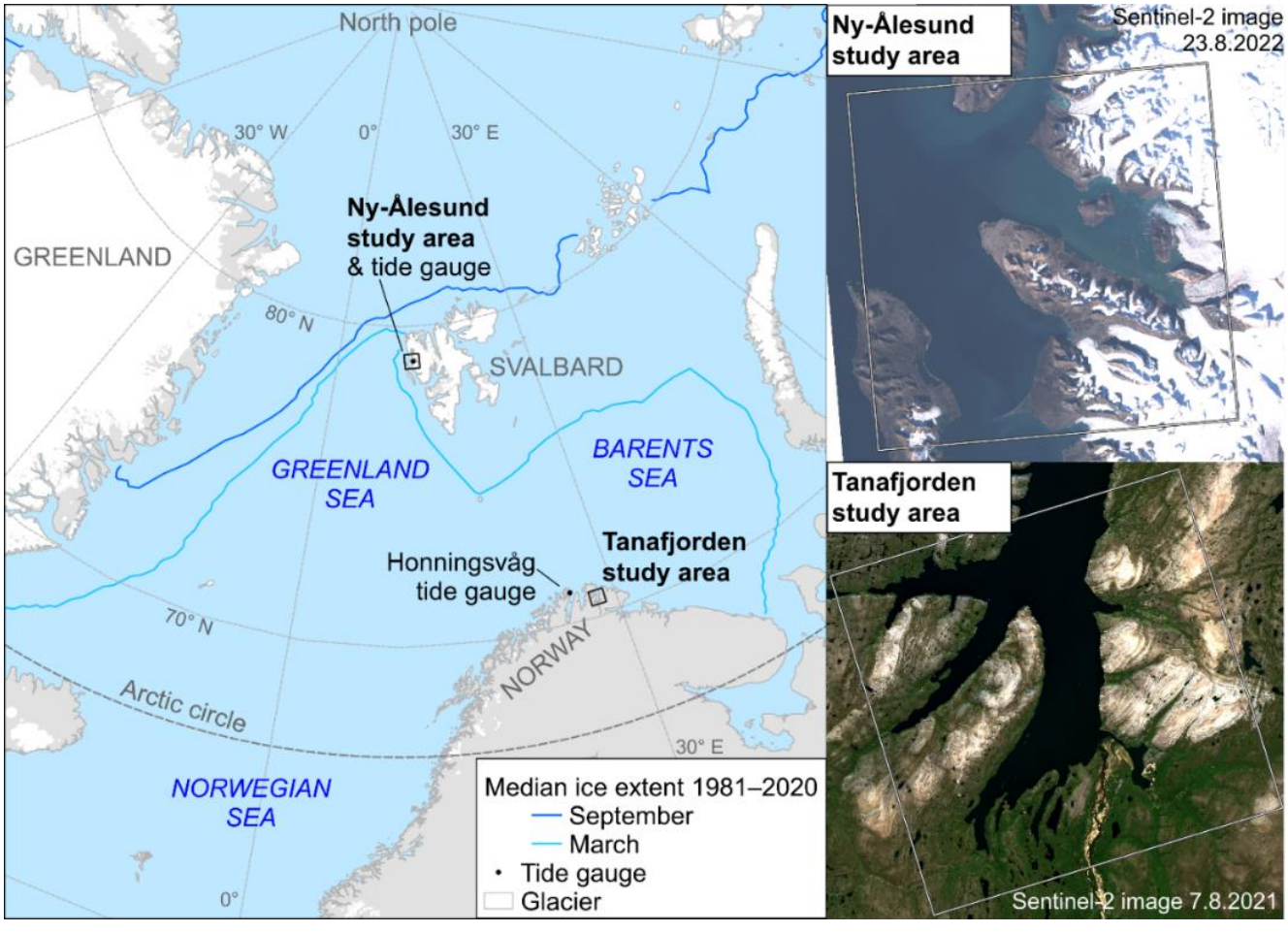

Figure 2. The two study areas: Tanafjorden in northern Fennoscandia, the Norwegian Barents Sea coast, and Ny-Ålesund in the high-arctic Svalbard. The size of each study area is 2500 km² (50 km * 50 km in the local UTM coordinate reference system). Spatial data: National Snow and Ice Data Center and Copernicus Sentinel.

2.2 Validation data of modern shoreline

Independent validation data were created to examine the accuracy of the land cover classification and shoreline detection. Two types of validation data were created, both corresponding to mean sea level conditions during c. 2019–2022. First, the shorelines of the study areas (Figure 2) were digitized by hand at a 1/5000 scale. Second, the coastal zones (excluding lakes and ponds) of the two study areas were randomly sampled, creating 2000 validation points in each study area, and manually

https://doi.org/10.5194/egusphere-2023-1399
Preprint. Discussion started: 12 September 2023

classified into land and sea. These validation data were created by the same coastal geomorphologist to maximize the homogeneity of the data. The interpretations were mainly based on hand-picked remote sensing images. For Tanafjorden, the interpretation was also based on in-situ observations from October 2021. The validation data are described in detail in the Supplement.

3 Results

Results of the final procedure are reported in this paper, whereas results of the main iterations, namely single-sensor approaches and alternative classification algorithms, are reported in the Supplement.

3.1 Data availability

The final procedure processed a total of 624 images of the Tanafjorden study area and 625 images of the Ny-Ålesund study area (see Supplement for details). For Tanafjorden, more than 30 images were available for each time-step. The availability until 2013 was notably lower for Ny-Ålesund, and there were only 6–16 images available for three early five-year time-steps, namely 1984–1988, 1994–1998 and 2004–2008. After calculating the number of observations on each pixel, these three image collections were considered too small for reliable time-step summaries (Table 1). Still, there was enough data to create a shoreline time series with five time-steps and covering a time period of 30 years. For this paper, we manually checked the possibility of including the lower-quality tier 2 Landsat 5 and Landsat 7 images to increase the number of observations but found that their quality was not sufficient. Due to the short revisit time of the Sentinel-2 mission, particularly in high latitudes, the number of available images was high in both study areas from 2017 onward.

For the most recent time-step, there were at least 26 observations and up to 332 observations on each pixel (Table 1; Figure 3). For the first six time-steps, and particularly for Ny-Ålesund, there were notable areas with less than five valid observations on a pixel (Figure 3). Being below the observation count threshold (≥ 5), these pixels were masked from the time-step summary, creating local gaps in the time series. In Tanafjorden, most of those were mountain tops with patches of snow that melt very late in the summer (Figure 3). The pixel quality algorithm (Landsat CFMASK) often falsely classified them as clouds. The same general pattern of observation counts was visible throughout the time series in Tanafjorden. It was evident that the existing cloud detection algorithms unnecessarily decreased data availability, while using a cloud mask was necessary for the outcome. In Ny-Ålesund, the spatial distribution of the data shortages was more random, depending on tile divisions (Figure 3).

https://doi.org/10.5194/egusphere-2023-1399
Preprint. Discussion started: 12 September 2023

Table 1. The minimum and maximum number of observations on individual pixels for each time-step and study area. Time-steps 1984–1989, 1994–1998 and 2004–2008 were excluded altogether from the Ny-Ålesund time series due to a generally low number of observations.

	Tanafjorden		Ny-Ålesund	
Time-step	**Min**	**Max**	**Min**	**Max**
1984–1988	1	36	(0	4)
1989–1993	0	24	1	15
1994–1998	0	18	(0	7)
1999–2003	0	28	2	15
2004–2008	0	41	(0	10)
2009–2013	0	46	2	23
2014–2018	7	82	24	100
2019–2022	26	104	46	332

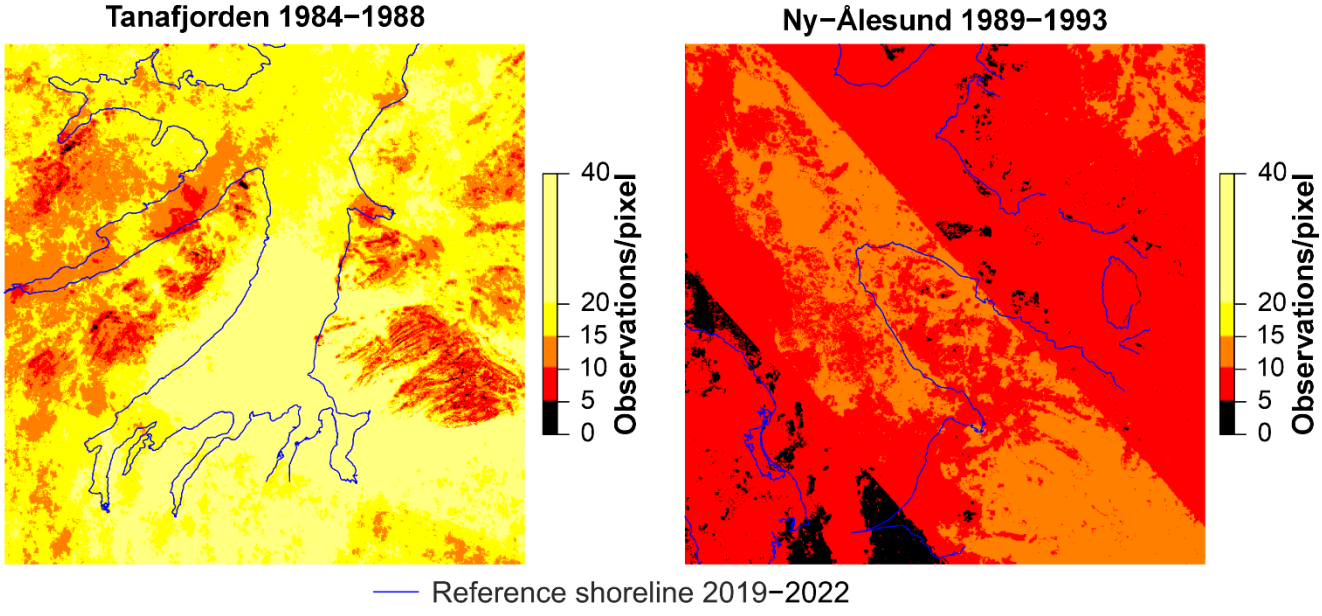

Figure 3. The spatial distribution of observation counts for the first available time-step for the two study areas. Pixels with fewer than five observations are highlighted in black and were masked from the time-step summary.

The procedure required observations from at least five satellite images to make decisions about each pixel and time-step. This decision fusion efficiently reduced noise and accounted for some of the short-term variations in sea level, caused by tides and weather conditions. The efficiency of the noise reduction was sensitive to the observation count, and thus increasing satellite image availability increased the reliability of the decision. The median sea level of single time-steps ranged between –60 and 0 cm, while sea levels in individual images varied between –170 and 100 cm (Figure 4A). This

https://doi.org/10.5194/egusphere-2023-1399
Preprint. Discussion started: 12 September 2023

meant that the extracted land cover and shoreline data reflected the long-term average conditions much better than data extracted from individual images would have.

In the Tanafjorden satellite image collection, the median sea level was particularly high during time-steps 1984–1988, 1989–1993 and 2004–2008 and particularly low during 1999–2003 and 2014–2018 (Figure 4A). Despite the high number of observations since 2017, the median sea level difference between the last two time-steps was as large as 42 cm. Undoubtedly, the remaining sea level differences between time-steps might have influenced the location of the extracted shoreline, at least in flat meso-tidal areas like the Tana River delta. Some of the time-step differences reflected more general interannual differences and sea level trends. The annual mean sea levels of Tanafjorden varied between years for almost 20 cm (Figure 4B), while the trend was weak ($p(t) = 0.027$). In Ny-Ålesund, there was a clear regressive trend ($p(t) < 0.001$) and the long-term relative sea level dropped more than 20 cm during the examined 39 years (Figure 4B). This sea level drop was clearly reflected in the satellite image collections for the Ny-Ålesund study area (Figure 4A). In other words, sea level differences in the Ny-Ålesund satellite image collection partly reflected long-term changes in sea level, but the impact of short-term sea level variations was also notable.

https://doi.org/10.5194/egusphere-2023-1399
Preprint. Discussion started: 12 September 2023

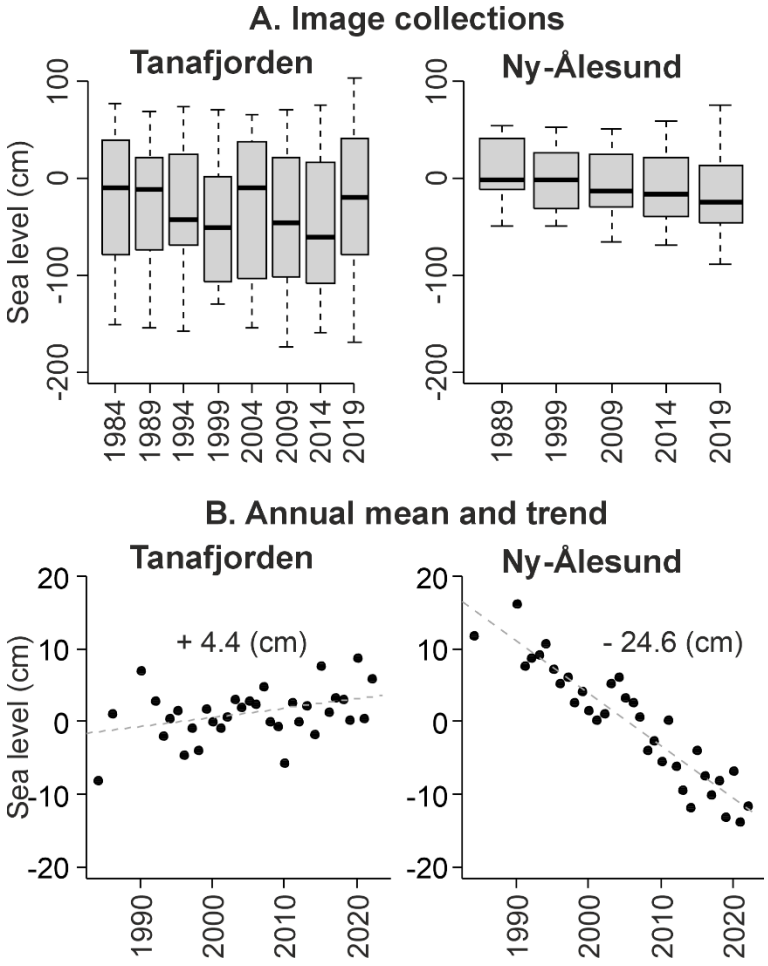

Figure 4. (A) Sea levels at the acquisition time of satellite images and (B) the annual mean sea levels in the two study areas. The linear trends and total mean sea level changes during the 39-year period are shown in B. The Tanafjorden sea levels are calculated from data of the Honningsvåg mareograph (Figure 2). Sea levels are reported relative to the mean sea level in 1996–2014. Sea level data: Norwegian Mapping Authority, Hydrographic Service.

3.2 Accuracy of classification and shorelines

Validation of the coastal land cover outputs for the time-step 2019–2022 against the independent set of 2000 coastal points showed that the procedure reached an overall classification accuracy of over 99 % in both study areas (Table 2). There were more misclassified water points in Tanafjorden and more misclassified land points in Ny-Ålesund (Table 2). In the Tanafjorden study area, the remaining misclassified points were located very close (in practice all < 30 meters) to the actual shoreline, in intertidal zones, and in areas shadowed by mountains (Figure 5A). In the Ny-Ålesund study area, many misclassified points were also located very close to the shoreline, but the largest errors were centred in areas with moving glacier margins (Figure 5B).

https://doi.org/10.5194/egusphere-2023-1399
Preprint. Discussion started: 12 September 2023

The median error distance from the reference shoreline to the modelled shoreline was less than 15 meters in both study areas, which is roughly half of the Landsat image pixel size of 30 meters (Table 2). In Tanafjorden, the longest error distances were found either in intertidal zones – most of them located in estuaries – or in mountain shadows (Figure 5C). The single largest error distances were obtained in Ny-Ålesund (Table 2). The longest error distances mainly occurred in ice-marginal areas, but some also occurred in the lagoon of Richardlaguna on the island of Prins Karls Forland and at a pier in the town of Ny-Ålesund (Figure 5D). Outside these challenging areas, however, the error distances were generally smaller in Ny-Ålesund than in Tanafjorden.

Validation results for the single-sensor outputs and alternative classification algorithm outputs are reported in the Supplement. We also examined the impact of five environmental factors on the classification accuracy of two best-performing algorithms, namely NDWI and random forest, to help improve the procedure. These five factors were sediment type, distance to the reference shoreline, primary productivity measured with NDVI, slope, and illumination. The results (see Supplement for details) indicated that the final iterations should aim at improving classification accuracy in mountain shadows, shallow sandy areas, and coastal water with high loads of suspended sediment. Areas near glacier margins and built coastlines were also found problematic, but fixing these problems was beyond the scope of this paper.

Table 2. Land cover classification accuracy and shoreline error distances of the final procedure for the time-step 2019–2022. Classification accuracies are examined against an independent set of 2000 coastal points in each study area.

Classification accuracy	**Tanafjorden**	**Ny-Ålesund**
Overall accuracy	0.994	0.991
Misclassified water points	10 (1.2 %)	4 (0.4 %)
Misclassified land points	3 (0.3 %)	15 (1.6 %)
Shoreline error distances (m)		
Median error distance	13.6	9.1
95 % quantile	78.9	156.8

https://doi.org/10.5194/egusphere-2023-1399
Preprint. Discussion started: 12 September 2023

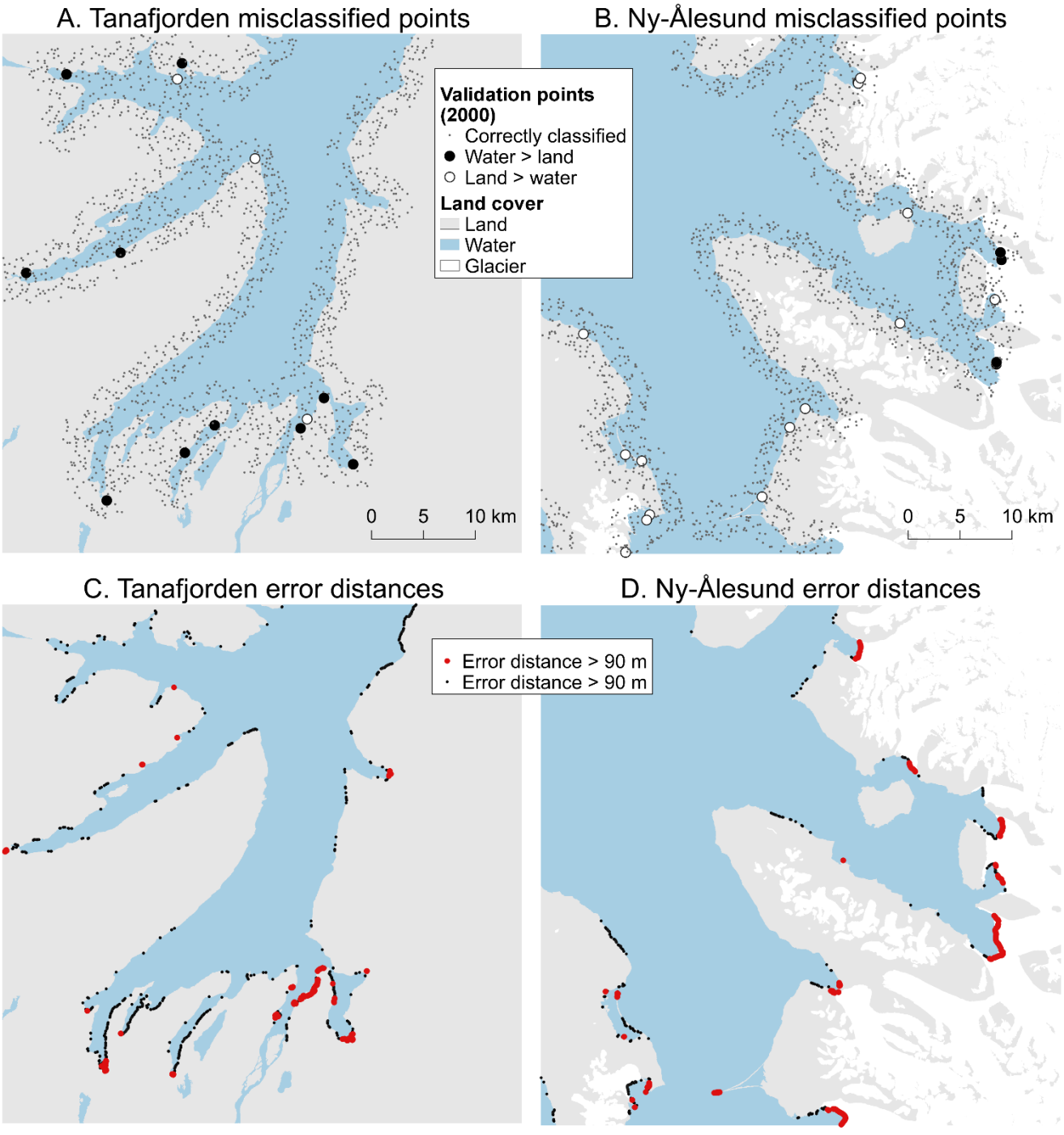

Figure 5. (A–B) Distribution of the misclassified points and (C–D) shoreline error distances for the time-step 2019–2022 in the two study areas. Glacier extents: Norwegian Polar Institute, Svalbard basic map 1:100 000.

https://doi.org/10.5194/egusphere-2023-1399
Preprint. Discussion started: 12 September 2023

3.3 Examples of geomorphological applications

The procedure was mainly designed to identify areas where coastal change intensity is high at the pan-Arctic or regional scale, but also to enable the examination of the most distinct changes at the local scale. Hence, the outputs can be used for coastal geomorphological analyses in the Arctic at regional and local scales. To exemplify some of the possibilities, seven summary variables were calculated from the final land cover time series. These were the probability to belong to the water class, the long-term trend, the change intensity, the first and last time-steps in the water class, and the first and last time-steps in the land class (Figure 6 and further description in Supplement). The seven variables can be used at the regional scale to detect hotspots of coastal change, erosion, and accretion, either manually or automatically. We were able to find such hotspots in both study areas. They were related to the Tana River delta in Tanafjorden and the ice-margin coasts near Ny-Ålesund (Figure 6). We also showed how the results provided information with sufficient spatial resolution (30 m) to study local-scale processes along the coast. Zooming in on the dynamic Tana River delta, we were able to see the gradual erosion of the banks and upstream sand bars and the corresponding accumulation in the downstream direction (Figure 6A). We could also detect the rapid retreat of the ocean-terminating glaciers in north-western Svalbard and the 400-meter spit accretion north of the Richardlaguna (Figure 6B).

https://doi.org/10.5194/egusphere-2023-1399
Preprint. Discussion started: 12 September 2023

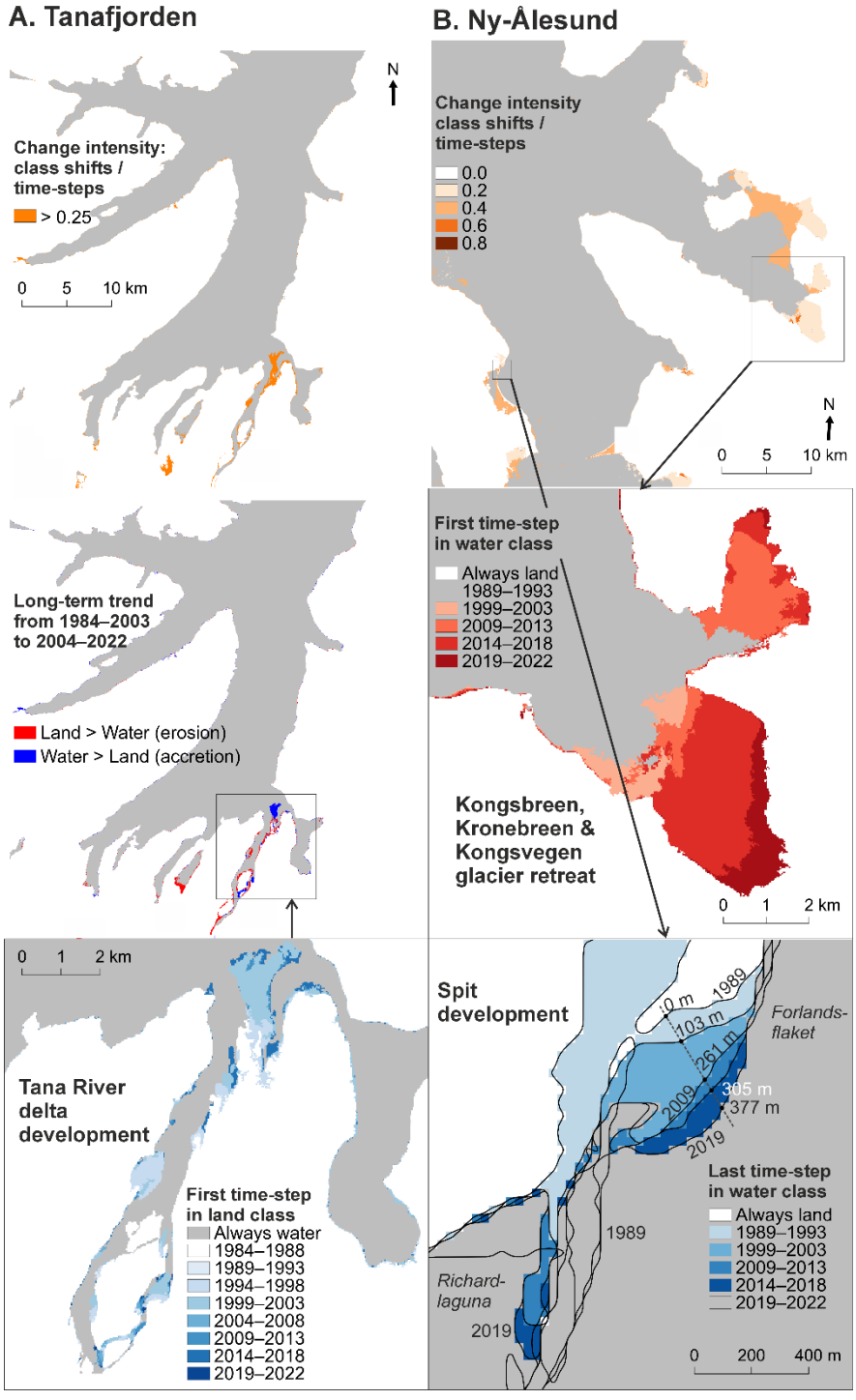

Figure 6. Examples of time series summary variables for geomorphological applications in the (A) Tanafjorden and (B) Ny-Ålesund study areas. Both regional and local-scale examples are given. The development of the highly active Tana River delta, the retreat of three marine-terminating glaciers in north-western Svalbard, and the development of a spit north of the Richardlaguna are clearly visible from the data.

https://doi.org/10.5194/egusphere-2023-1399
Preprint. Discussion started: 12 September 2023

4 Conclusions

We propose a new automated procedure for mapping long-term shoreline displacement anywhere in the Arctic and for large areas at a time. The outputs of the procedure include a time series of coastal land cover (land and sea; raster data) and a shoreline time series (vector data).

The approach utilizes cloud computing in Google Earth Engine to overcome the problem of processing the high number of open satellite images needed to cover large areas and the entire satellite image coverage period of c. 40 years. We show that for one 2 500 km² area of interest, the procedure utilizes c. 600 satellite images to create coastal land cover and shoreline time series in less than one hour. However, low data availability tends to create local gaps in the time series.

We demonstrate that such a level of accuracy in such diverse environments could not be reached without utilizing complementary spatial data, and decision fusion. The procedure applies data fusion (including sensor fusion, algorithm fusion and decision fusion) to improve classification accuracy and processing efficiency. Data fusion accelerates computations and reduces problems related to the low availability and quality of satellite data in the Arctic before 2013. Decision fusion across five-year time-steps reduces the impacts of noise like clouds and cloud shadows and short-term changes like tidal sea level fluctuations.

The procedure has been iteratively developed and validated in two contrasting study areas in the Arctic Norway, namely the meso-tidal Tanafjorden in the Norwegian low Arctic and the glaciated, micro-tidal coast around Ny-Ålesund in Svalbard. Validation in these two study areas indicates an overall classification accuracy of more than 99 % and a median shoreline error distance of less than 15 m in 2019–2022. Local terrain complexity and differences in sea water quality have an impact on classification accuracy. The remaining errors are concentrated in mountain shadows, shallow sandy areas, coastal water with high loads of suspended sediment, glacier margins and built coastlines. It might be possible in the future to overcome these challenges by involving more specific spatial data in the procedure. The procedure will be made more applicable to coasts that are surrounded by all-year sea ice. Namely, we will in the future adopt a three-class land cover classification with classes land, water, and ice. It is also evident that accuracy is sensitive to the availability of remote sensing data. While not tested in this paper, we assume that the classification accuracy is lower and shoreline error distances are longer before 2013 than during the last two time-steps due to lower data availability.

We exemplify how the procedure provides new information for identifying coastal change hotspots at the regional scale. This information can be used to locate coasts that are particularly prone to shoreline displacement in the future. The coastal land cover time series can also be used for examining long-term trends. The spatial resolution of the output product is 30 meters, corresponding to the resolution of the Landsat time series. This can be considered a sufficient resolution for examining some of the most distinct local-scale processes in the Arctic, such as coastal erosion, glacier retreat, and the development of sandy coastlines. We show how the retreat of the marine-terminating glaciers becomes visible in high-arctic Svalbard and how one of the largest Fennoscandian deltas has developed in the last 30 years. We are confident that the

https://doi.org/10.5194/egusphere-2023-1399
Preprint. Discussion started: 12 September 2023

procedure can be applied to any coastal study area in and beyond the Arctic. We particularly look forward to producing the first circumpolar dataset of shoreline displacement.

Code and data availability

Code for the procedure for creating long-term Arctic shoreline displacement time series is available upon request at the time of the submission of the manuscript. The code will be openly available via Zenodo as soon as the project for creating the first circumpolar shoreline displacement dataset is completed. The spatial output and validation data produced for this paper, together with code for calculating the summaries and shorelines are available via Zenodo (Nylén et al., 2023).

Supplement

A full methodological description of the procedure and previous iterations, and more detailed results are available as a Supplement document for this paper: add link.

Author contribution

TN designed the study consulting MCN and CGI. TN did field work. TN and CGI developed the code. TN and MCN designed the validation procedure, the time series summaries and visualisations. TN analysed and visualised the result for the paper and prepared the manuscript with contributions from all co-authors.

Competing interest

The authors declare that they have no conflict of interest.

Acknowledgement

TN was funded by the Academy of Finland: project ARIMPA, grant number 343338. MC was funded by the Turku Collegium for Sciences, Medicine and Technology (TCSMT).

References

AMAP: Arctic climate change update 2019: An update to key findings of snow, water, ice and permafrost in the Arctic (SWIPA) 2017, Arctic Monitoring and Assessment Programme (AMAP), Oslo, Norway, 12 pp., https://www.amap.no/documents/download/3295/inline, 2019.

https://doi.org/10.5194/egusphere-2023-1399
Preprint. Discussion started: 12 September 2023

Are, F., Reimnitz, E., Grigoriev, M., Hubberten, H. W., and Rachold, V.: The influence of cryogenic processes on the erosional Arctic shoreface, J. Coast. Res., 24, 110–121, doi:10.2112/05-0573.1, 2008.

Barnhart, K. R., Overeem, I., and Anderson, R. S.: The effect of changing sea ice on the physical vulnerability of Arctic coasts, Cryosphere, 8, 1777–1799, doi:10.5194/tc-8-1777-2014, 2014.

Bendixen, M. and Kroon, A.: Conceptualizing delta forms and processes in Arctic coastal environments, Earth Surf. Process. Landf., 42, 1227–1237, doi:10.1002/esp.4097, 2017.

Bishop-Taylor, R., Nanson, R., Sagar, S., and Lymburner, L.: Mapping Australia's dynamic coastline at mean sea level using three decades of Landsat imagery, Remote Sens. Environ., 267, 112734, https://doi.org/10.1016/j.rse.2021.112734, 2021.

Bourriquen, M., Baltzer, A., Mercier, D., Fournier, J., Pérez, L., Haquin, S., Bernard, E., and Jensen, M.: Coastal evolution and sedimentary mobility of Brøgger Peninsula, northwest Spitsbergen, Polar Biol., 39, 1689–1698, doi:10.1007/s00300-016-1930-1, 2016.

Ding, Y., Yang, X., Jin, H., Wang, Z., Liu, Y., Liu, B., Zhang, J., Liu, X., Gao, K., and Meng, D.: Monitoring coastline changes of the Malay Islands based on Google Earth Engine and dense time-series remote sensing images, Remote Sens., 13, 3842, https://doi.org/10.3390/rs13193842, 2021.

Farquharson, L. M., Mann, D. H., Swanson, D. K., Jones, B. M., Buzard, R. M., and Jordan, J. W.: Temporal and spatial variability in coastline response to declining sea-ice in northwest Alaska, Mar. Geol. 404, 71–83, doi:10.1016/j.margeo.2018.07.007, 2018.

Günther, F., Overduin, P. P., Sandakov, A. V., Grosse, G., and Grigoriev, M. N.: Short- and long-term thermo-erosion of ice-rich permafrost coasts in the Laptev Sea region, Biogeosciences, 10, 4297–4318, doi:10.5194/bg-10-4297-2013, 2013.

Hollesen, J., Callanan, M., Dawson, T., Fenger-Nielsen, R., Friesen, T. M., Jensen, A. M., Markham, A., Martens, V. V., Pitulko, V. V., and Rockman, M.: Climate change and the deteriorating archaeological and environmental archives of the Arctic, Antiquity, 92, 573–586, doi:10.15184/aqy.2018.8, 2018.

Irrgang, A. M., Lantuit, H., Gordon, R. R., Piskor, A., and Manson, G. K.: Impacts of past and future coastal changes on the Yukon coast - threats for cultural sites, infrastructure, and travel routes, Arct. Sci., 5, 107–126, doi:10.1139/as-2017-0041, 2019.

Ismail, M. A., Waqas, M., Ali, A., Muzzamil, M. M., Abid, U., and Zia, T.: Enhanced index for water body delineation and area calculation using Google Earth Engine: a case study of the Manchar Lake, J. Water Clim. Chang., 13, 557–573, doi:10.2166/wcc.2021.282, 2022.

Laengner, M. S., Siteur, K., and van der Wal, D.: Trends in the seaward extent of saltmarshes across Europe from long-term satellite data, Remote Sens., 11, 1653, doi:10.3390/rs11141653, 2019.

Lantuit, H., Overduin, P. P., Solomon, S., and Mercier, D.: Coastline dynamics in polar systems using remote sensing, Environmental Science Engineering and Technology, Nova Publishers, 174 pp., ISBN 978-1-61668-140-1, 2010.

Lantuit, H., Overduin, P. P., Couture, N., Wetterich, S., Are, F., Atkinson, D., Brown, J., Cherkashov, G., Drozdov, D., Forbes, D. L., Graves-Gaylord, A., Grigoriev, M. N., Hubberten, H. W., Jordan, J., Jorgenson, T., Odegard, R. S., Ogorodov,

https://doi.org/10.5194/egusphere-2023-1399
Preprint. Discussion started: 12 September 2023

S., Pollard, W. H., Rachold, V., Sedenko, S., Solomon, S., Steenhuisen, F., Streletskaya, I., and Vasiliev, A.: The Arctic Coastal Dynamics database. A new classification scheme and statistics on arctic permafrost coastlines, Estuaries Coast., 35, 383–400, doi:10.1007/s12237-010-9362-6, 2012.

Lantuit, H. and Pollard, W. H.: Fifty years of coastal erosion and retrogressive thaw slump activity on Herschel Island, southern Beaufort Sea, Yukon Territory, Canada, Geomorphology, 95, 84–102, doi:10.1016/j.geomorph.2006.07.040, 2008.

Larsen, J. N. and Fondahl, G. (Eds.): Arctic human development report – Regional processes and global linkages, Nordic Council of Ministers, 504 pp., ISBN 978-92-893-3883-7, 2014.

Li, J., Knapp, D. E., Lyons, M., Roelfsema, C., Phinn, S., Schill, S. R., and Asner, G. P.: Automated global shallow water bathymetry mapping using Google Earth Engine, Remote Sens., 13, 1469, https://doi.org/10.3390/rs13081469, 2021.

Li, J., Ma, R., Cao, Z., Xue, K., Xiong, J., Hu, M., and Feng, X.: Satellite detection of surface water extent: A review of methodology, Water 14, 1148, doi:10.3390/w14071148, 2022.

Nylén, T., Calle-Navarro, M., Gonzales-Inca, C.: Arctic shoreline displacement and validation data for two pilot study areas, doi:10.5281/zenodo.7993787, 2023.

Overeem, I., Anderson, R. S., Wobus, C. W., Clow, G. D., Urban, F. E., and Matell, N.: Sea ice loss enhances wave action at the Arctic coast, Geophys. Res. Lett., 38, L17503, doi:10.1029/2011GL048681, 2011.

Pérez-Cutillas, P., Pérez-Navarro, A., Conesa-García, C., Zema, D. A., and Amado-Álvarez, J. P.: What is going on within google earth engine? A systematic review and meta-analysis, Remote Sens. Appl.: Soc. Environ., 29, 100907, https://doi.org/10.1016/j.rsase.2022.100907, 2023.

Radosavljevic, B., Lantuit, H., Pollard, W., Overduin, P., Couture, N., Sachs, T., Helm, V., and Fritz, M.: Erosion and flooding-threats to coastal infrastructure in the Arctic: A case study from Herschel Island, Yukon Territory, Canada, Estuaries Coast., 39, 900–915, doi:10.1007/s12237-015-0046-0, 2016.

Serreze, M. C. and Barry, R. G.: Processes and impacts of Arctic amplification: A research synthesis, Glob. Planet. Change, 77, 85–96, doi:10.1016/j.gloplacha.2011.03.004, 2011.

Vos, K., Harley, M. D., Splinter, K. D., Simmons, J. A., and Turner, I. L.: Sub-annual to multi-decadal shoreline variability from publicly available satellite imagery, Coast. Eng., 150, 160–174, doi:10.1016/j.envsoft.2019.104528, 2019.

Zagórski, P., Rodzik, J., Moskalik, M., Strzelecki, M. C., Lim, M., Blaszszyk, M., Prominska, A., Kruszewski, G., Styszynska, A., and Malczewski, A.: Multidecadal (1960-2011) shoreline changes in Isbjornhamna (Hornsund, Svalbard), Pol. Polar Res., 4, 369–390, doi:10.1515/popore−2015−0019, 2015.